Journal for Multiscale Computational Engineering, 8(2), xxx–xxx (2010)

A MOLECULAR MECHANICS STUDY ON THE EFFECT OF SURFACE MODIFICATION ON THE INTERFACIAL PROPERTIES IN CARBON NANOTUBE/POLYSTYRENE NANOCOMPOSITES

Dong Qian,[1,*] Peng He,[2] & Donglu Shi[3]

[1]*Department of Mechanical Engineering, University of Cincinnati, Cincinnati, OH 45221-0072, USA*

[2]*Universal Energy System, Inc., 4401 Dayton-Xenia Dr., Dayton, OH 45432-1894, USA*

[3]*Department of Chemical and Materials Engineering, University of Cincinnati, Cincinnati, OH 45221-0012, USA*

[*]Address all correspondence to Dong Qian E-mail: dong.qian@uc.edu

We have developed a molecular mechanics approach to study surface modification and its effect on the mechanics of interfaces in nanocomposites. Investigation of this topic is motivated by the exceptional mechanical properties that have been demonstrated in a new generation of nanomaterials. The systems studied mainly include polystyrene polymers that are reinforced by carbon nanotubes subjected to different surface modifications. The interactions among the atoms in the system are governed by the empirical potentials in the form of force fields. To directly probe the interfacial mechanics, a nanotube pull-out test is simulated. The interfacial properties between the carbon nanotube and polystyrene matrix are evaluated from the numerical experiments under different surface modification conditions. The simulation results show that both the interfacial energy and interfacial shear stress can be improved significantly by introducing a functional group on the surface of the carbon nanotube. Interfacial strength up to 486 MPa can be achieved with the employed surface modification. The simulation also indicates the existence of an optimum functional ratio in terms of the energy barrier for interfacial sliding.

KEY WORDS: *carbon nanotubes, nanocomposites, surface modification, molecular dynamics, polymer matrix, polystyrene*

1. INTRODUCTION

Since its discovery in 1991, the carbon nanotube (CNT) has been widely studied as a new generation of nanomaterial. Besides the potential of being applied in sensors, field emission, and other devices, another research direction is using CNTs as reinforcing materials for composite applications due to the combination of their high strength and lightweight properties. One of the major obstacles to using CNT as a polymer filler is the weak adhesion (interfacial properties) between the CNT and the polymer matrix. Without good adhesion, the external load could not be transferred from the polymer matrix to the CNT efficiently (Mokashi et al., 2007). In other words, the excellent mechanical properties of the CNT could not be fully utilized if the interfacial properties between the CNT and the polymer matrix are too weak. Therefore, much research has focused on improving the adhesion between the CNT and polymer matrix using a surface modification approach and understanding the interaction between the surface-modified CNT and the polymer matrix.

In a general context, the interfacial properties of CNT-based composites have been investigated in a number of modeling studies (Lordi and Yao, 2000; Liao and Li,

1543–1649/2010/$35.00 © 2010 by Begell House, Inc.

2001; Frankland et al., 2002; Frankland and Harik, 2003; Frankland et al., 2003; Griebel and Hamaekers, 2004; Mylvaganam and Zhang, 2004; Namilae and Chandra, 2005; Liu, Xiao et al., 2007; Namilae et al., 2007) using an atomistic simulation approach. Specific topics such as elastic properties, interfacial strength based on pull-out tests, and load transfer mechanisms are discussed. In the case of pristine CNT embedded in a polymer matrix, interfacial strengths are observed to be in the range of 18–135 MPa. The interfacial mechanics between functionalized CNTs and the polymer matrix have been investigated (Frankland, 2002; Namilae and Chandra, 2005; Liu et al., 2007; Namilae et al., 2007) using a molecular dynamics approach. Due to the large variations in the surface modification in terms of both the functional species and functional ratio, interfacial strengths in a relatively wide range (50–500 MPa) have been reported. However, a major limitation with use of the molecular dynamics approach is the time scale associated with the loading condition, which is typically on the order of pico-seconds. Correspondingly, the imposed loading rates in these cases are very high and it is difficult to directly verify the pull-out simulation. For instance, it has been shown that the computed interfacial shear stress is strongly dependent on the loading rate (Frankland and Harik, 2003). In this paper, we developed a molecular mechanics approach in which an equilibrium solution is obtained for the pull-out test. Compared with the molecular dynamic simulation, the solution is not affected by the loading rate and is compatible with the typical pull-out experiment, which is quasi-static in nature.

In terms of the selection of the material system, there are several experimental techniques widely used to modify the surface of CNTs to improve interfacial properties in CNT nanocomposites, such as the solution oxidation method (Ajayan et al., 1993; Ebbesen, 1996; Esumi et al., 1996; Sekar and Subramanian, 1996; Colomer et al., 1998; Yumura, Ohshima et al., 1999; Hernadi et al., 2001; Jeong et al., 2001; Mann and Hase, 2001; Moon et al., 2002; Feng et al., 2003; Gajewski et al., 2003; Leonhardt et al., 2003; Xu et al., 2004), sidewall functionalization method (Holzinger et al., 2001; Hirsch, 2002; Tagmatarchis et al., 2002; Peng et al., 2003; Dyke and Tour, 2004; Kang, 2004; Banerjee et al., 2005; Wu and Shi, 2005), fluorination method (Hamwi et al., 1997; Mickelson et al., 1999; Kudin et al., 2001; An, Heo et al., 2002; Lebedev et al., 2003; Kawasaki et al., 2004; Khare et al., 2004), and high-energy radical bombardment (Ni and Sinnott, 2000; Lim et al., 2003; Pomoell et al., 2004). Previous experimental studies on the interfacial properties have yielded conflicting results. Generally there seems to be two classes of observations: one concludes that the load transfer is weak, such as in Schadler et al. (1998) and Ajayan et al. (2000). The other groups of experiments (Wagner et al., 1998; Cooper et al., 2002) have reported very high interfacial strengths (300–500 MPa). The discrepancies in the experimental data are largely due to the combination of processing conditions for surface modification of the CNT and the synthesis process of the nanocomposites. These discrepancies highlight the importance of using a modeling approach to study the nature of the interface, which could provide invaluable insights on the fundamental mechanisms.

To mimic the experimental procedure, we consider systems of CNT that are either pristine or surface modified. The functional species are assumed to be covalently bonded to the CNT surface. The interaction between the surface-modified CNT and polymer matrix is governed by the van der Waals type of interaction. The interface being studied in this paper is similar to that of intertube interactions in the case of nanotube ropes (Qian et al., 2003) in which a Lennard–Jones potential developed earlier (Qian et al., 2001) was used. For the system being studied here, we propose that there are two fundamental mechanisms that account for the load transfer: The first is the frictional effect due to the surface roughness of the CNT and polymer. The functional species and the rough interface of the polymer provide energy barriers that prevent the interfacial sliding. The second is the energy cost to create the free surface. Such a free surface could take place as the polymer matrix might contain voids. For the simulation to be presented, we mainly focus on the first mechanism. In our previous studies, we demonstrated plasma deposition of a thin polymer film on the surfaces of CNTs [46] and used the coated nanotubes to reinforce a polystyrene matrix [47]. In this paper, the interfacial properties and mechanical properties of this particular material system are studied by computational approaches. A similar material system has also been studied by Liao and Li (2001). The major difference here is the size of the system and the additional surface modification considered in this paper. Comparisons with the results in Liao and Li (2001) are presented.

In addition to the influence of surface modification on interfacial strength, a highly related topic is the effect of the functionalization on the mechanical properties of the CNTs themselves. For instance, a modeling study (Garg and Sinnott, 1998) has indicated that surface modification could degrade the mechanical properties of the CNTs such as stiffness and strength. Although this effect is not being specifically dealt with in the present paper, its

contribution to the interfacial mechanics is directly represented by the molecular model. For the functional ratio we tested (up to a moderate 2%), we speculate that the degradations in the mechanical properties are insignificant in terms of their effect on the CNT/polymer interface. However, a separate study is needed to verify this proposition.

The rest of the paper is organized as follows: we first describe the basic simulation setup in Section 2, including structure generation, interatomic potential, and loading conditions. We then present and discuss the results in terms of the interfacial strength and interfacial energy calculations. Final conclusions are made in Section 4.

2. SIMULATION CONCEPTS AND SETUP

Molecular simulation has been proven to be an extremely useful tool in that it can provide direct insight into material and bulk phenomenon. There are several simulation methods available, such as ab initio (or first principles), Monte Carlo simulation, molecular dynamics, and molecular mechanics. In this research, molecular mechanics is used to investigate the interfacial properties between the polymer matrix and CNT. As the term indicates, molecular mechanics is different from conventional and widely used molecular dynamics methods. In molecular mechanics, the system is solved based on equilibrium. The potential energy of the system is minimized with respect to the atomistic degrees of freedom. The system is in equilibrium at the end of every simulation step and a new set of atomic positions is obtained during the minimization. At equilibrium, the energy of the system is at the minimum based on the force field used to represent the molecular interactions. The force field for a molecular system can be defined as a set of interatomic potentials required and parameterized to represent the physical system as accurately as possible. For a complex structure, involving multiple types of molecules interacting with each other, the force field also incorporates intermolecular and short-range potentials. The potential functions, their derivatives, and parameterization govern the equilibrium in molecular mechanics. To obtain an equilibrium solution, energy minimization based on the L-BFGS-B (Byrd, 1995) minimization algorithm, found to be robust for constrained and unconstrained problems, is used throughout our study. The pull-out simulations presented in this study are modeled by a quasi-static, displacement update scheme. The DL_POLY (Smith and Forester, 1996) software package was modified to incorporate the energy minimization scheme to implement the molecular mechanics scheme.

2.1 Force Fields and Molecular Potentials

In the case of our composite systems, CNTs and polystyrene are two distinct molecules with different sets of properties and definitions. A combination of various interatomic and intermolecular potentials is used for representing the composite systems.

The expression for the total energy of nanotube–polystyrene composite system is written as

$$E_{total} = E_{CNT} + E_{polymer} + E_{intermolecular} \quad (1)$$

in which E_{total} is the total energy of the system, E_{CNT} is the potential energy of the CNT, $E_{polymer}$ is the energy of the polymer matrix, and $E_{intermolecular}$ is the energy of interaction between the CNT and the polymer matrix. The potential energy models for these components are described in subsequent sections.

2.2 Potential Model for CNTs

The empirical bond order potential proposed by Brenner (Brenner, 1990) is used for modeling CNTs in either pristine or functionalized forms. This potential is formulated for covalent systems and leads to accurate representation of graphite-like systems. The potential energy equation for Brenner potential is given as

$$E_b = \sum_i \sum_{j(>i)} \left[V_R\left(r_{ij}\right) - \overline{B}_{ij} V_A\left(r_{ij}\right) \right] \quad (2)$$

where $V_R\left(r_{ij}\right)$ and $V_A\left(r_{ij}\right)$ are the repulsive and attractive terms as follows:

$$V_R\left(r_{ij}\right) = \frac{f_{ij}\left(r_{ij}\right) D_{ij}^{(e)}}{\left(S_{ij}-1\right)} e^{-\sqrt{2S_{ij}}\beta_{ij}\left(r-R_{ij}^{(e)}\right)} \quad (3)$$

$$V_A\left(r_{ij}\right) = \frac{f_{ij}\left(r_{ij}\right) D_{ij}^{(e)} S_{ij}}{\left(S_{ij}-1\right)} e^{-\sqrt{2/S_{ij}}\beta_{ij}\left(r-R_{ij}^{(e)}\right)} \quad (4)$$

in which $D_{ij}^{(e)}$, S_{ij}, β_{ij}, and $R_{ij}^{(e)}$ are constants, formulated for each atom in the covalent bond. The equation for $f_{ij}\left(r_{ij}\right)$, a smooth cutoff function which accounts for bond stretching and breaking, is given below.

$$f_{ij}(r) = \begin{cases} 1, \quad r < R_{ij}^{(1)} \\ \left[1 + \cos\left(\dfrac{\pi\left(r - R_{ij}^{(1)}\right)}{\left(R_{ij}^{(2)} - R_{ij}^{(1)}\right)}\right)\right]/2, \\ R_{ij}^{(1)} < r < R_{ij}^{(2)} \\ 0, \quad r > R_{ij}^{(2)} \end{cases} \tag{5}$$

Here $R_{ij}^{(1)}$ and $R_{ij}^{(2)}$ are cutoff lengths corresponding to bond stretching and breaking, respectively. $\overline{B}_{ij}$, the bond order term, is an average of the terms associated with each atom participating in the bond and a correction term F_{ij}, primarily dependent on the number of bonds each, made by atoms i and j.

$$\overline{B}_{ij} = (B_{ij} + B_{ji})/2 + F_{ij}\left(N_i^{(t)}, N_j^{(t)}, N_{ij}^{conj}\right) \tag{6}$$

$$\begin{aligned} B_{ij} = \Bigg[1 + \sum_{k(\neq i,j)} G_i(\theta_{ijk}) f_{ik}(r_{ik}) \\ \times e^{\alpha_{ijk}\left[\left(r_{ij} - R_{ij}^{(e)}\right) - \left(r_{ik} - R_{ik}^{(e)}\right)\right]} \\ + H_{ij}\left(N_i^{(H)}, N_i^{(C)}\right)\Bigg]^{-\delta_i} \end{aligned} \tag{7}$$

The function $G_i(\theta)$ is given below with c_0 and d_0 constants, and θ is the angle between two adjacent covalent bonds of atom i.

$$G_C(\theta) = a_0\left\{1 + \frac{c_0^2}{d_0^2} - \frac{c_0^2}{\left[d_0^2 + (1 + \cos\theta)^2\right]}\right\} \tag{8}$$

For the specific parameterization of the modeling constants, we refer to Brenner (1990) for details.

2.3 Force Field for Polymers

The polymer systems are modeled using DL_POLY force field. The DL_POLY force field representation of polymer incorporates four interatomic potentials: bond, valence angle, dihedral angle, and 1–4. The only intermolecular potential accounted for is the short-range (van der Waals) potential. Electrostatic (coulombic) forces are ignored. The total energy of the polystyrene matrix can be expressed as

$$\begin{aligned} E_{polyethylene} = E_{bond} + E_{angle} + E_{dihedral} \\ + E_{short-range} \end{aligned} \tag{9}$$

The terms in the above expression are explained in the form of the following potential equations from the DL_POLY force field.

a) Bond (Morse potential):

$$E(r_{ij}) = E_0\left[\left\{1 - e^{(-k(r_{ij} - r_0))}\right\}^2 - 1\right] \tag{10}$$

where r_{ij} is the bond length, E_0 and k are constants, and r_0 is the equilibrium bond length. The parameters used for various bonds are listed in Table 1.

b) Valence angle (harmonic cosine potential):

$$E(\theta_{jik}) = \frac{k}{2}\left(\cos(\theta_{jik}) - \cos(\theta_0)\right)^2 \tag{11}$$

where $\theta_{jik}$is the angle between the two bonds, *k* is a constant, and $\theta_0$is the equilibrium value of the angle. The parameters used for the various valence angles in the system are given in Table 2.

c) Dihedral angle (cosine potential):

$$E(\phi_{ijkn}) = A\left[1 + \cos(m \cdot \phi_{ijkn} - \delta)\right] \tag{12}$$

in which ϕ_{ijkn} is the dihedral angle, and A, m and δ are constants. The parameter values used for all the dihedral interactions are given in Table 3. In addition to these parameters, two more parameters are used to control the nonbonded forces acting between the 1st and the 4th atoms defining the dihedral. These interactions are called 1–4 interactions and use the same potentials defined for the rest of the short-range interactions. These potentials are described in the next section.

2.4 Interaction Model between CNTs and Polymer

The DL_POLY force field incorporates potentials for nonbonded as well as intermolecular interactions. The complete definition of the force field for polystyrene includes nonbonded interactions between the polymer atoms. In our system, the only interactions between the two materials are the nonbonded or van der Waals (vdW) forces. Algorithms to generate van der Waals interaction lists are incorporated in DL_POLY to simulate double-walled nanotube and graphite systems in a separate study. Lennard–Jones (Lennard-Jones, 1929) (L-J) potential is the potential of choice for all vdW interactions in our system. L-J parameters reported by Girifalco (Girifalco and Lad,

TABLE 1: Parameters for bond (Morse) potential

Parameter	C–C bond	C–H bond	Units
E_0	70.000	70.000	kcal/mol
r_0	1.53	1.09	Å
k	2.236	2.236	$(\text{Å})^{-1}$

TABLE 2: Parameters for valence angle (harmonic cosine) potential

Parameter	C–C–C	H–C–H	C–C–H/H–C–C	Units
k	112.5	112.5	112.5	kcal/mol
θ_0	109.47	109.47	109.47	rad

TABLE 3: Parameters for dihedral angle (cosine) potential

Parameter	H–C–C–H/H–C–C–C (terminal C atom)	C–C–C–H/C–C–C–C (internal C atom)	Units
A	0.1667	0.1111	kcal/mol
δ	0	0	rad
m	3	3	-

1956) for carbon–carbon systems are used for all vdW interactions involving carbon atoms. The L-J potential equation is given below:

$$U\left(r_{ij}\right) = 4\varepsilon\left[\left(\frac{\sigma}{r_{ij}}\right)^{12} - \left(\frac{\sigma}{r_{ij}}\right)^{6}\right] \tag{13}$$

where r_{ij} is the distance between the nonbonded pair of atoms, and ε and σ are constants. The form of the L-J potential in Eq. (13) can be simplified and written as

$$U\left(r_{ij}\right) = \left[\frac{A}{\left(r_{ij}\right)^{12}} - \frac{B}{\left(r_{ij}\right)^{6}}\right] \tag{14}$$

The parameters A and B used for different atom-pair combinations are reported in Table 4 below.

2.5 Atomic Structures

The nanocomposite systems studied in this research are based on single-walled nanotubes embedded in an amorphous polystyrene matrix. In the first step, a random walk algorithm implemented in DL_POLY's Java Graphic User Interface (GUI) is modified to generate the amorphous polystyrene structure. In this process, the polymer chain starts with a single methane unit. One hydrogen atom from each unit is replaced by the carbon atom from another coming unit to propagate the chain. Unlike the algorithm in the original DL_POLY for polyethylene generation, the difference in the backbone atom attachment is carefully considered for polystyrene. The atom is divided into two groups. One group is (CH_2). For this group of backbone atoms, no special change is made. Another group of backbone carbon atoms is connected with the benzene ring. For this group of atoms, one hydrogen atom is substituted by the benzene ring. The coordinates of this benzene ring are generated according to the vector which points from the backbone carbon atom to the hydrogen atom that is substituted.

Each added carbon unit is verified to be energetically stable and not overlapping with any of the previous units. Unlike polyethylene, the side group of polystyrene, i.e., the benzene ring, is much larger compared with the hydrogen atom. In certain cases, the random chain propagation may be stopped due to the large space barrier. In these cases, the energy barrier is reduced so that the random chain can be further propagated. A typical composite cell is shown in Fig. 1.

The connectivity algorithm is crucial to the proper definition of the polymer force field. The algorithm implemented in DL_POLY is divided into two main parts—generating the bond connectivity and defining the force field functions and parameters. The bonds are generated based on interatomic distances, and the original logic is slightly modified to sort the bonds based on atom numbers. The bond list is further traversed to define the valence angle and dihedral interactions. Finally, the inter-

TABLE 4: Parameters for L-J potential

Interaction type	Parameter	
	A(kcal/mol Å^{12})	B(kcal/mol Å^{6})
C–C	802442.06	460.584
C–H	150602.42	151.339
H–H	17198.63	32.337

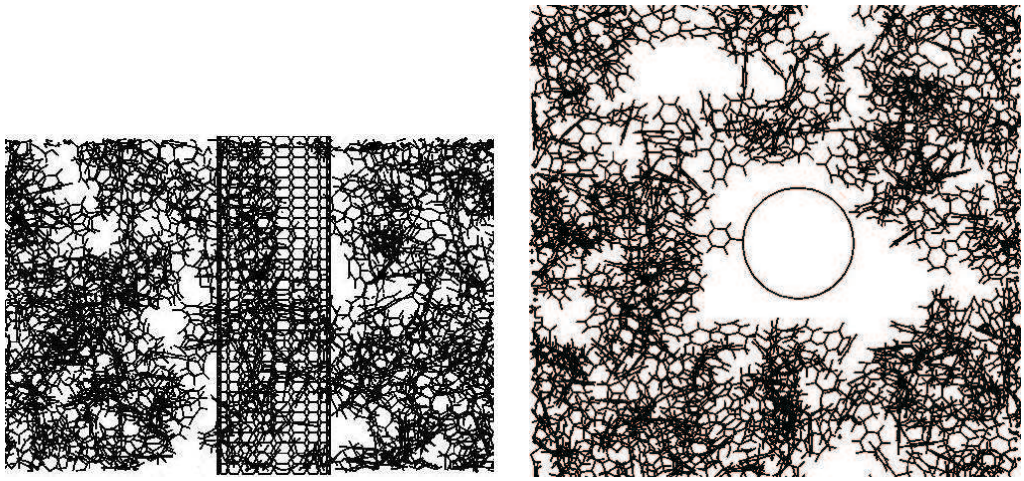

(a) (b)

FIG. 1: Composite with through CNT in amorphous polystyrene **(a)** Longitudinal **(b)** Transverse

atomic potential corresponding to each bond, angle, and dihedral interaction is selected and the parameters are generated. An important part of this logic is finding the hybridization and neighbors of the carbon atoms and selecting the potentials and parameters accordingly. For example, a carbon atom bonded to three hydrogen atoms and one carbon has slightly different constants from a carbon bonded to two hydrogen and two carbons.

2.6 Simulation Setup

A pull-out test is a standard test used to determine the interfacial properties and load transfer capabilities between reinforced material and the polymer matrix. For glass fiber or carbon fiber reinforced composite (the size is around 10–100 μm), a pull-out experiment can be carried out by applying force on an individual fiber, then pushing or pulling this fiber out of the sockets. The loading history is recorded to analyze the interfacial mechanics. To model CNT pull-out, boundary conditions similar to the experimental test are applied. The specific implementation is discussed in the next section.

2.6.1 Atomic Structures and Boundary Conditions

All the composite systems studied for interfacial properties are based on a through armchair (10,10) CNT with 700 carbon atoms inside an amorphous polystyrene matrix enclosed in a cell of $65 \times 65 \times 40$ Å. The amorphous polystyrene matrix has a total of 12,002 atoms. An illustration of the pull-out process is shown in Fig. 2. The incremental axial displacement is imposed on 20 car-

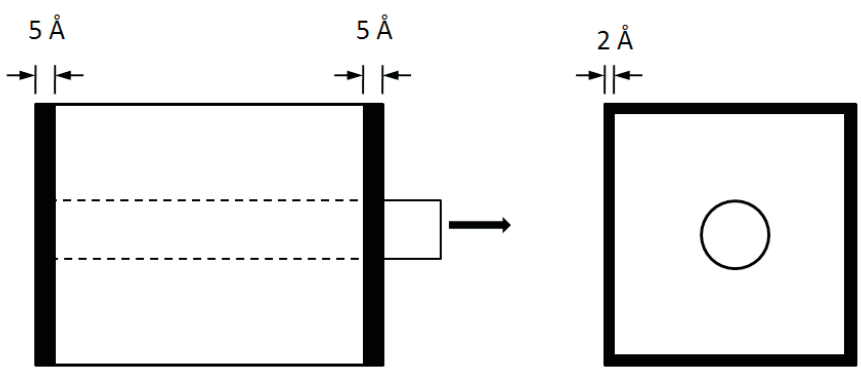

FIG. 2: Illustration of CNT pullout

bon atoms at the tip of the CNT. For the amorphous polystyrene matrix, a 5 Å slab of polymer atoms is fixed on the front and back sides (shaded area in Fig. 2) during the loading process. An additional 2 Å slab of polymer atoms is also fixed on each of the four sides in the cross-section plane (Fig. 2).

The location of the functional sites on the CNT is controlled mainly by a statistical uniform distribution. In addition, two rules are followed during the functional sites generation:

(1) No atom at the end of CNT is functionalized. The range is 2 Å. This rule ensures that the functional sites are embedded in the polystyrene matrix.

(2) No more than two functional groups are attached on the neighbor carbon atoms. During the plasma modification, when one atom on the CNT surface is active and absorbs one functional group, the benzene ring, the large space barrier prevents the neighbor carbon atoms from absorbing another benzene ring.

An example of a (10,10) tube functionalized by benzene is shown in Fig. 3.

The functional ratio of a CNT, which is defined as the number of carbon atoms connected with the functional groups divided by the total number of carbon atoms, changes from 0 to 2%. More specifically, four cases of CNTs corresponding to different surface modification conditions are simulated. These cases are summarized in Table 5. No higher functional ratio is simulated because 2% is almost the highest value that can be obtained in the experiment (He et al., 2006).

2.6.2 Pull-Out Simulation Setup

During the simulation, incremental displacement is imposed at one end of the CNT, then the energy is minimized at each incremental pull-out step to arrive at equilibrium. This process continues until the entire CNT is removed from the polystyrene matrix. In the present simulation, a displacement of 0.005 Å per step is carried out until the complete pull-out is accomplished. Figure 4 shows images of the nanotube pull-out process. To evaluate the interfacial mechanics, two measures have been developed. One is the "average" interfacial shear stress obtained by dividing the shear force at the nanotube/polystyrene interface by the entire nanotube surface area. The second one is the "local" interfacial shear stress by evaluating the shear force corresponding to the two translational CNT unit cells (40 atoms) in the middle of the CNT and then dividing it by the equivalent surface area. Use of the average shear stress gives an overall estimate of the load transfer, while the local shear stress provides some indication of the tube/polymer matrix interaction at the local level.

TABLE 5: A summary of the functional ratio and number of functional sites

Functional ratio	0	0.003	0.01	0.02
The number of functional site	0	2	7	14

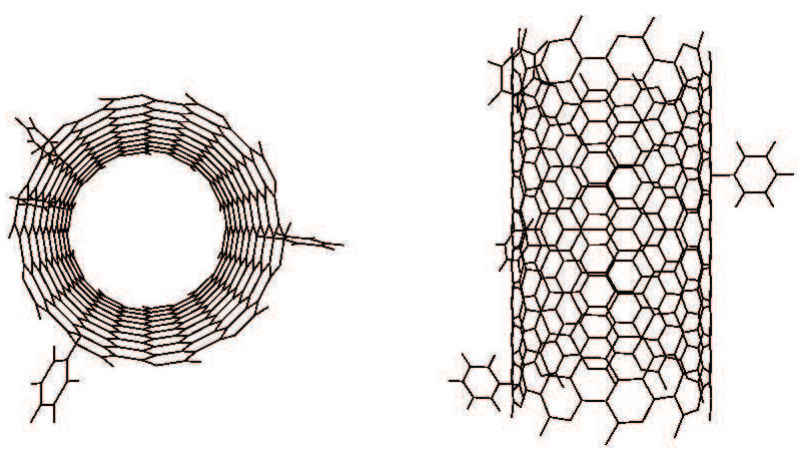

FIG. 3: The structure of benzene funcionalized (10, 10) armchair carbon nanotube (Functional sites: 4)

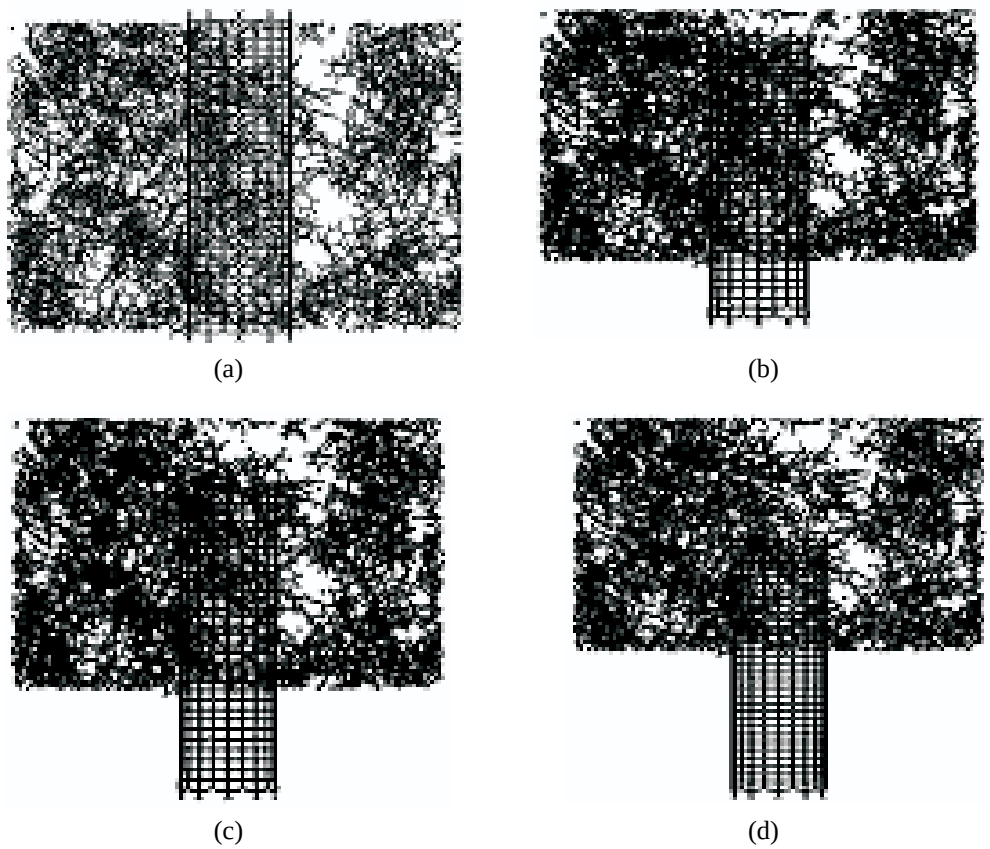

FIG. 4: Sanpshots of nanotube pull-out process

3. SIMULATION RESULT

Figures 5–8 show the average and local interfacial shear stresses for both the pristine CNT and surface-modified CNT. For the surface-modified tube, the number of functional sites is seven in this case.

As can be seen in Figs. 5 and 6, both the average and local shear stresses change in almost periodical patterns when no surface modification is involved. In addition, they reduce to zero when the imposed CNT tip displacement is larger than 50 Å. (At this moment, the entire CNT is removed from polystyrene matrix). The shear stress during the pull-out also shows a negative sign, an indication that the shear force is opposite to the pull-out direction. In contrast, the shear stress history of the functionalized CNT (Figs. 7 and 8) shows a dramatic difference. The periodical feature of the shear stress history is no longer preserved and large positive shear stress values are shown in Figs. 7 and 8. As mentioned before, the size of the benzene ring is much larger than the size of the hydrogen atom. Subsequently, it becomes a space barrier during the pull-out simulation. When the benzene ring functional group passes the region where it was originally trapped, the interfacial force acting on it becomes repulsive and this leads to a switch from pull to push at the interface. As shown in the shear stress history curve, the positive range can be clearly observed because of this pull-to-push change. Unlike the smooth surface of the original CNT with periodically arranged atoms, the surface of the functional CNT becomes rough because of the attached benzene ring. As such, the random roughness destroys the periodical surface pattern, leading to a random shear force history during the pull-out process.

In order to study the effect of functional density on interfacial shear stress, the maximum shear stress corresponding to the total CNT surface is evaluated during the pull-out cases for different functional ratios. The reason for choosing the maximum shear stress value is that, without overcoming this obstacle, the CNT could not be pulled out from polystyrene matrix. Therefore, we define this

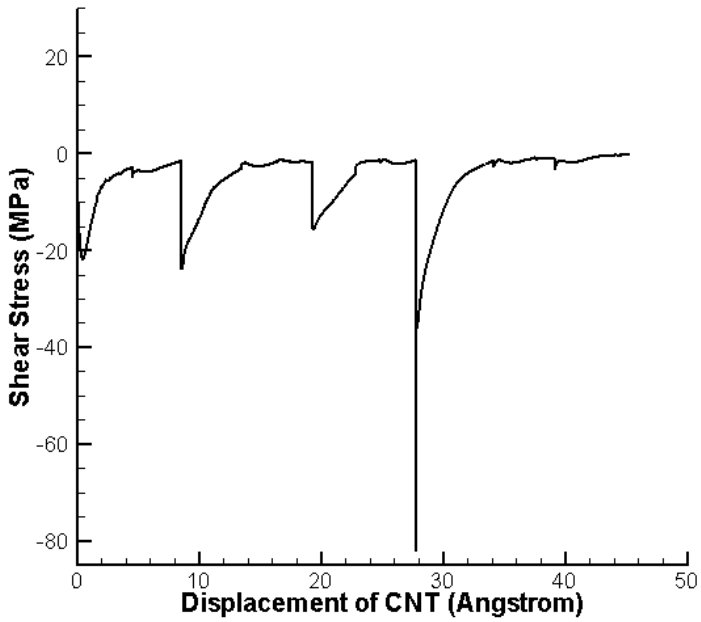

FIG. 5: Shear stress computed based on entire carbon nanotube (pristine CNT)

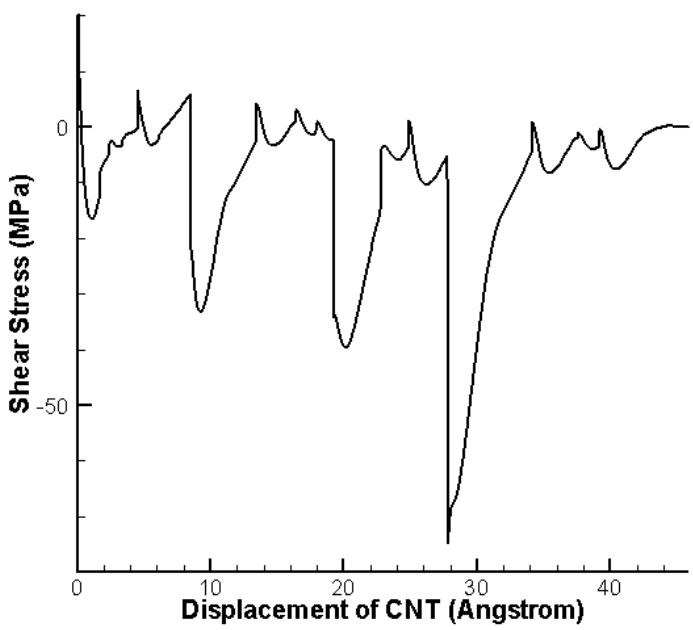

FIG. 6: Shear stress computed based on middle layer of carbon nanotube (pristine CNT)

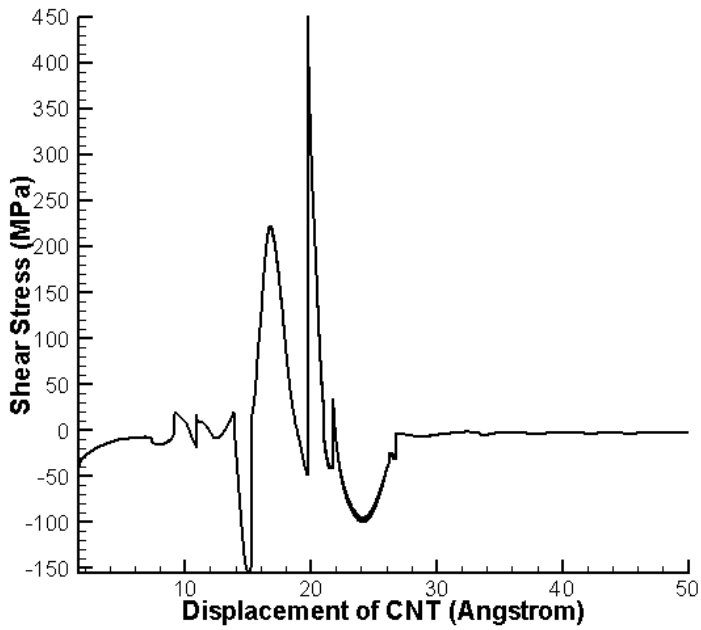

FIG. 7: Shear stress acted on entire carbon nanotube (modified CNT)

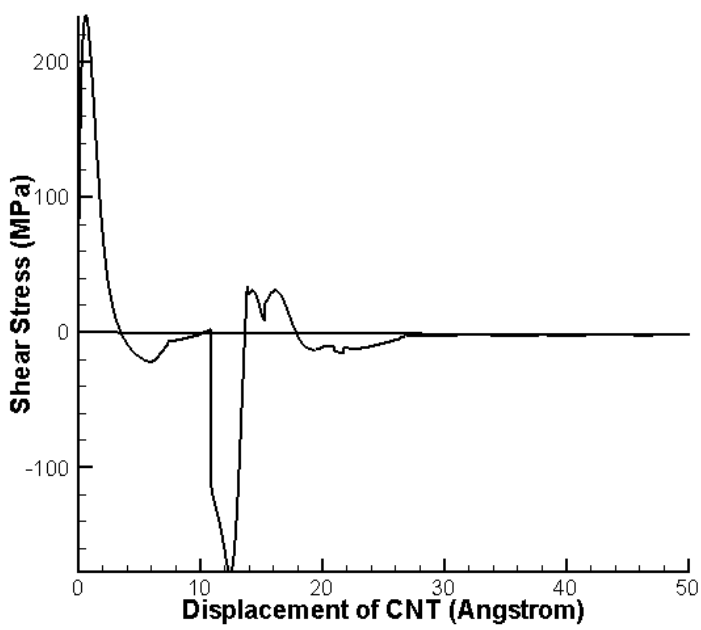

FIG. 8: Shear stress acted on middle layer of carbon nanotube (modified CNT)

maximum shear stress as the shear strength of the interface. Figure 9 shows the shear strength as a function of number of functional sites. It is clearly seen that the maximum shear force increases dramatically with the increase of the functional ratio.

Compared with the pristine CNT, the shear strength is observed to increase up to 6.3 times when the functional site increases to 14, which corresponds to a functional ratio of 2%. This result indicates the benefit of attaching a functional group on the surface of the CNT at a moderate functional ratio and further explains the improvements in the mechanical properties. In terms of the comparison with the experimental data, we note that the shear strength value at 2% is 486 MPa, which is on the same order of magnitude as observed in Cooper et al. (2002) (366 MPa) and Wagner et al. (1998) (500 MPa). For the pristine tube, our computed value of 72 MPa is smaller than the shear strength of 160 MPa presented in the modeling work of Liao and Li (2001). This difference is mainly contributed by the length of the tube, which leads to different mechanisms of interfacial shear. In Liao and Li (2001), their CNT length is approximately 20 Å. As a result, the energy needed to create a free surface during the pull-out plays a more important role than the frictional effect due to the relatively short contact length. In our work, the tube length is about three times longer and the frictional effect is a more important contributing factor. Finally, we note that a different force field is used in Liao and Li (2001) which could also lead to the differences.

In order to find out the effect of functional ratio on the energy, the energy after 200 steps relaxation is used as a reference for the composite system. The maximum energy value obtained during the pull out is used as another value to calculate the energy barrier for pull-out, which is essentially the difference between the two. As can be seen in Fig. 10, the energy barrier keeps increasing with the increasing functional density.

In terms of the basic trend, the value of the energy barrier increases significantly when the number of functional sites increases from 0 to 7 (1%). However, when the number of the functional sites is further increased to 14 (a functional density of 2%), no appreciable improvement can be found. This phenomenon can be qualitatively interpreted as follows: When the functional ratio is low, one functional group addition will seriously change the roughness of the CNT surface. At this range, the energy barrier for pull-out will be increased rapidly. But when the density reaches certain value (1% in this study), fur-

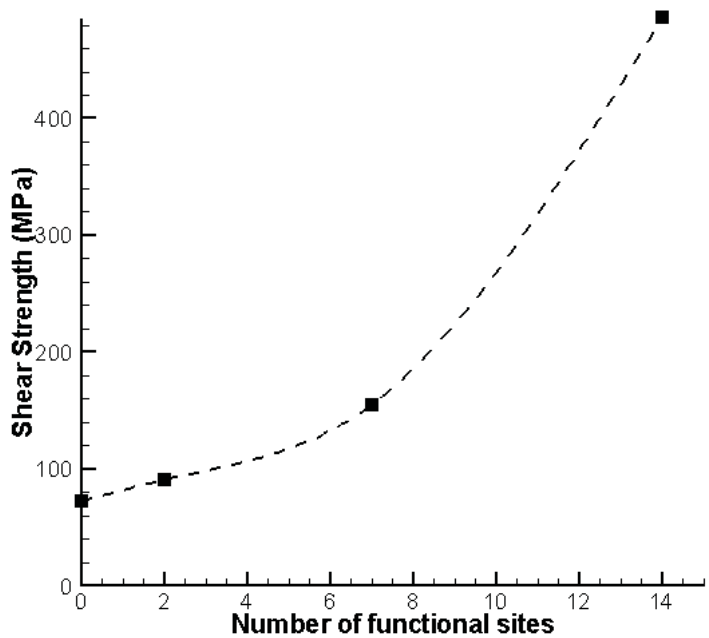

FIG. 9: Maximum shear force vs Number of functionalized sites

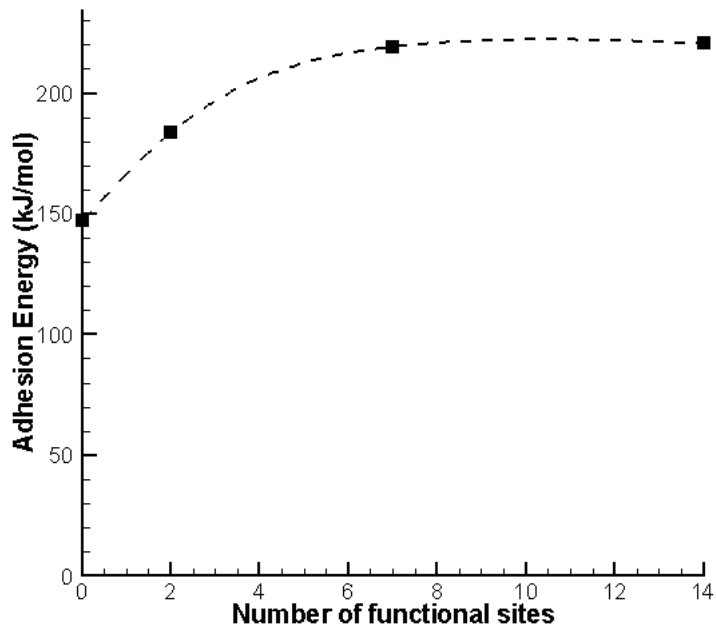

FIG. 10: The pull-out obstacle energy vs. number of functionalized sites

ther increasing the functional group will prevent the close interaction between the CNT and polymer matrix. As a result, it reduces the energy barrier for pull-out. It is noted that the same trend is not reflected in the shear stress as shown in Fig. 9. This because the average shear stress can be approximated as the energy barrier divided by the average sliding distance to overcome this energy barrier. With the increasing functional ratio, the average sliding distance to overcome an energy barrier will reduce. In our simulation, the combined effects yield an increasing shear stress at the interface.

For the case of a pristine tube, we obtain an energy threshold value of 147 kcal/mol. We note that Liao and Li (2001) quoted an adhesion energy value of 158.7 kcal/mol. Although this is close to the energy barrier we obtained, the two energy terms have different meanings. From a mechanics viewpoint, the adhesion energy provides a measure of the surface energy difference between a completely embedded CNT and isolated CNT. In contrast, the energy barrier used in this paper indicates the maximum variation in the surface energy during the pull-out process. For most applications involving CNT-based nanocomposites, the sliding at the CNT/polymer interface is unlikely to create a significant amount of free surface. As such, the energy barrier is a more suitable measure of the interfacial load transfer for nanocomposites. In summary, interfacial properties of CNTs can be improved by introducing a functional group on the surface of the CNT. However, there is an optimum surface functional density as far as the energy barrier for sliding is concerned.

4. CONCLUSION AND SUMMARY

In this paper, the pull-out of a surface-modified CNT embedded in polystyrene matrix is successfully simulated by using a molecular mechanics approach. The DL-POLY force field for polystyrene matrix and Brenner potential for CNT are integrated to compute the energy and force history as a function of load. The interfacial properties between the CNT and the polystyrene matrix are evaluated for both pristine and a CNT functionalized by benzene molecules. The numerical results show that both interfacial energy and interfacial shear stress can be improved by introducing a functional group on the surface of the CNT.

The numerical result provides a useful theoretic model for future surface modification experiments. In addition, the interfacial strength computed can be further cast in the

form of a cohesive law which enables large-scale simulation of CNT-based nanocomposites at the continuum level (Liu et al., 2008).

The present work has only partially succeeded in revealing the possibility of improving dispersion and adhesion of CNTs by polymerization. There are still some important issues requiring further investigation, such as the selection of better monomers and the study of chemical reactions actually occurring during the coating process. The computational framework presented in this paper can be extended to perform further studies on these topics.

ACKNOWLEDGEMENTS

Dong Qian acknowledges general support from the National Science Foundation (grants CMMI 0600583 and 0700107). Any opinions, findings, conclusions, or recommendations expressed in these documents are those of the author(s) and do not necessarily reflect the views of the National Science Foundation.

REFERENCES

Ajayan, P. M., Ebbesen, T. W., Ichihashi, T., Iijima, S., Tanigaki, K., and Miura, M., Opening carbon nanotubes with oxygen and implications for filling, *Nature*, vol. **362**(6420), p. 522, 1993.

Ajayan, P. M., Schadler, L. S., Giannaris, C., and Rubio, A., Single-walled carbon nanotube-polymer composites: Strength and weakness, *Adv. Mater*., vol. **12**(10), 750–753, 2000.

An, K. H., Heo, J. G., Jeon, K. G., Bae, D., Jo, C. S., Yang, C. W., Park, C. Y., Lee, Y. H., Lee, Y. S., and Chung, Y. S., X-ray photoemission spectroscopy study of fluorinated single-walled carbon nanotubes, *Appl. Phys. Lett*., vol. **80**(22), pp. 4235–4237, 2002.

Banerjee, S., Hemraj-Benny, T., and Wong, S. S., Covalent surface chemistry of single-walled carbon nanotubes, *Adv. Mater*., vol. **17**(1), pp. 17–29, 2005.

Brenner, D. W., Empirical potential for hydrocarbons for use in simulating the chemical vapor-deposition of diamond films, *Phys. Rev. B*, vol. **42**(15), pp. 9458–9471, 1990.

Byrd, R. H., Lu, P. H., Nocedal, J., and Zhu, C. Y., A limited memory algorithm for bound constrained optimization, *SIAM J. Sci. Comput.*, vol. **16**(5), pp. 1190–1208, 1995.

Colomer, J. F., Piedigrosso, P., Willems, I., Journet, C., Bernier, C., Van Tendeloo, G., Fonseca, A., and Nagy, J. B., Purification of catalytically produced multiwall nanotubes, *J. Chem. Soc. Faraday Trans*., vol. **94**(24), pp. 3753–3758, 1998.

Cooper, C. A., Cohen, S. R., Barber, A. H., and Wagner, H. D., Detachment of nanotubes from a polymer matrix, *Appl. Phys. Lett.*, vol. **81**(20), pp. 3873–3875, 2002.

Dyke, C. A. and Tour, J. M., Overcoming the insolubility of carbon nanotubes through high degrees of sidewall functionalization, *Chemistry-A European J.*, vol. **10**(4), pp. 813–817, 2004.

Ebbesen, T. W., Wetting, filling and decorating carbon nanotubes, *J. Phys. Chem. Solids*, vol. **57**(6–8), pp. 951–955, 1996.

Esumi, K., Ishigami, M., Nakajima, A., Sawada, K., and Honda, H., Chemical treatment of carbon nanotubes, *Carbon*, vol. **34**(2), pp. 279–281, 1996.

Feng, Y. C., Zhou, G. M., Wang, G. P., Qu, M. Z., and Yu, Z. L., Removal of some impurities from carbon nanotubes, *Chem. Phys. Lett*., vol. **375**(5–6), pp. 645–648, 2003.

Frankland, S. J. V., Caglar, A., Brenner, D. W., and Griebel, M., Molecular simulation of the influence of chemical cross-links on the shear strength of carbon nanotube–polymer interfaces, *J. Phys. Chem. B*, vol. **106**(12), pp. 3046–3048, 2002.

Frankland, S. J. V. and Harik, V. M., Analysis of carbon nanotube pull-out from a polymer matrix, *Surf. Sci*., vol. **525**(1–3), pp. L103–L108, 2003.

Frankland, S. J. V., Harik, V. M., Odegard, G. M., Brenner, D. W., and Gates, T. S., The stress–strain behavior of polymer-nanotube composites from molecular dynamics simulation, *Compos. Sci. Technol*., vol. **63**(11), pp. 1655–1661, 2003.

Gajewski, S., Maneck, H. E., Knoll, U., Neubert, D., Dorfel, I., Mach, R., Strauss, B., and Friedrich, J. F., Purification of single-walled carbon nanotubes by thermal gas phase oxidation, *Diamond Relat. Mater.*, vol. **12**(3–7), pp. 816–820, 2003.

Garg, A. and Sinnott, S. B., Effect of chemical functionalization on the mechanical properties of carbon nanotubes, *Chem. Phys. Lett*., vol. **295**(4), pp. 273–278, 1998.

Girifalco, L. A. and Lad, R. A., Energy of cohesion, compressibility and the potential energy functions of the graphite system, *J. Chem. Phys.*, vol. **25**(4), pp. 693–697, 1956.

Griebel, M. and Hamaekers, J., Molecular dynamics simulations of the elastic moduli of polymer-carbon nanotube composites, *Comput. Methods Appl. Mech. Eng*., vol. **193**(17–20), pp. 1773–1788, 2004.

Hamwi, A., Alvergnat, H., Bonnamy, S., and Beguin, F., Fluorination of carbon nanotubes, *Carbon*, vol. **35**(6), pp. 723–728, 1997.

He, P., Gao, Y., Lian, J., Wang, L. M., Qian, D., Zhao, J., Wang, W., Schulz, M. J., Zhou, X. P., and Shi, D. L., Surface modification and ultrasonication effect on the mechanical properties of carbon nanofiber/polycarbonate compos-

ites, *Composites A*, vol. **37**(9), pp. 1270–1275, 2006.

Hernadi, K., Siska, A., Thien-Nga, L., Forro, L., and Kiricsi, I., Reactivity of different kinds of carbon during oxidative purification of catalytically prepared carbon nanotubes, *Solid State Ionics*, **141**, pp. 203–209, 2001.

Hirsch, A., Functionalization of single-walled carbon nanotubes, *Angew. Chem. Int. Ed.*, vol. **41**(11), pp. 1853–1859, 2002.

Holzinger, M., Vostrowsky, O., Hirsch, A., Hennrich, F., Kappes, M., Weiss, R., and Jellen, F., Sidewall functionalization of carbon nanotubes, *Angew. Chem. Int. Ed.*, vol. **40**(21), pp. 4002–4005, 2001.

Jeong, T., Kim, W. Y., and Hahn, Y. B., A new purification method of single-walled carbon nanotubes using H_2S and O^2 mixture gas, *Chem. Phys. Lett.*, vol. **344**(1–2), pp. 18–22, 2001.

Kang, H. S., Organic functionalization of sidewall of carbon nanotubes, *J. Chem. Phys.*, vol. **121**(14), pp. 6967–6971, 2004.

Kawasaki, S., Komatsu, K., Okino, F., Touhara, H., and Kataura, H., Fluorination of open- and closed-end single-walled carbon nanotubes, *Phys. Chem. Chem. Phys.*, vol. **6**(8), pp. 1769–1772, 2004.

Khare, B. N., Wilhite, P., and Meyyappan, M., The fluorination of single-wall carbon nanotubes using microwave plasma, *Nanotechnology*, vol. **15**(11), pp. 1650–1654, 2004.

Kudin, K. N., Bettinger, H. F., and Scuseria, G. E., Fluorinated single-wall carbon nanotubes, *Phys. Rev. B*, vol. **63**(4), art. no. -045413, 2001.

Lebedev, N. G., Zaporotskova, I. V., and Chernozatonskii, L. A., Fluorination of carbon nanotubes within the molecular cluster method, *Microelectron. Eng.*, vol. **69**(2–4), pp. 511–518, 2003.

Lennard-Jones, J. E., The electronic structure of some diatomic molecules, *Trans. Faraday Soc.*, vol. **25**, pp. 668–686, 1929.

Leonhardt, A., Ritschel, A., Kozhuharova, R., Graff, A., Muhl, T., Huhle, R., Monch, I., Elefant, D., and Schneider, C. M., Synthesis and properties of filled carbon nanotubes, *Diamond Relat. Mater.*, vol. **12**(3–7), pp. 790–793, 2003.

Liao, K. and Li, S., Interfacial characteristics of a carbon nanotube-polystyrene composite system, *Appl. Phys. Lett.*, vol. **79**(25), pp. 4225–4227, 2001.

Lim, H., Jung, H., and Joo, S. K., Control of carbon nanotube shape by ion bombardment, *Microelectron. Eng.*, vol. **69**(1), pp. 81–88, 2003.

Liu, J. Q., Xiao, T., Liao, K., and Wu, P., Interfacial design of carbon nanotube polymer composites: A hybrid system of noncovalent and covalent functionalizations, *Nanotechnology*, vol. **18**(16), pp. 165701–165701, 2007.

Liu, Y. J., Nishimura, N., Qian, D., Adachi, N., Otani, Y., and Mokashi, V., A boundary element method for the analysis of CNT/polymer composites with a cohesive interface model based on molecular dynamics, *Eng. Anal. Boundary Elem.*, vol. **32**(4), pp. 299–308, 2008.

Lordi, V. and Yao, N., Molecular mechanics of binding in carbon-nanotube-polymer composites, *J. Mater. Res.*, vol. **15**(12), pp. 2770–2779, 2000.

Mann, D. J. and Hase, W. L., Direct dynamics simulations of the oxidation of a single-wall carbon nanotube, *Phys. Chem. Chem. Phys.*, vol. **3**(19), pp. 4376–4383, 2001.

Mickelson, E. T., Chiang, I. W., Zimmerman, J. L., Boul, P. J., Lozano, J., Liu, J., Smalley, R. E., Hauge, R. H., and Margrave, J. L., Solvation of fluorinated single-wall carbon nanotubes in alcohol solvents, *J. Phys. Chem. B*, vol. **103**(21), pp. 4318–4322, 1999.

Mokashi, V. V., Qian, D., and Liu, Y. J., A study on the tensile response and fracture in carbon nanotube-based composites using molecular mechanics, *Compos. Sci. Technol.*, vol. **67**(3–4), pp. 530–540, 2007.

Moon, C. Y., Kim, Y. S., Lee, E. C., Jin, Y. G., and Chang, K. J., Mechanism for oxidative etching in carbon nanotubes, *Phys. Rev. B*, vol. **65**(15), pp. 155401–155404, 2002.

Mylvaganam, K. and Zhang, L. C., Chemical bonding in polyethylene-nanotube composites, A quantum mechanics prediction, *J. Phys. Chem. B*, vol. **108**(17), pp. 5217–5220, 2004.

Namilae, S. and Chandra, N., Multiscale model to study the effect of interfaces in carbon nanotube-based composites, *J. Eng. Mater. Technol.-Trans. ASME*, vol. **127**(2), pp. 222–232, 2005.

Namilae, S., Chandra, U., Srinivasan, A., and Chandra, N., Effect of interface modification on the mechanical behavior of carbon nanotube reinforced composites using parallel molecular dynamics simulations, *Comput. Model. Eng. Sci.*, vol. **22**(3), pp. 189–202, 2007.

Ni, B. and Sinnott, S. B., Chemical functionalization of carbon nanotubes through energetic radical collisions, *Phys. Rev. B*, vol. **61**(24), pp. R16343–R16346, 2000.

Peng, H. Q., Alemany, L. B., Margrave, J. L., and Khabashesku, V. N., Sidewall carboxylic acid functionalization of single-walled carbon nanotubes, *J. Am. Chem. Soc.*, vol. **125**(49), pp. 15174–15182, 2003.

Pomoell, J. A. V., Krasheninnikov, A. V., Nordlund, K., and Keinonen, J., Ion ranges and irradiation-induced defects in multiwalled carbon nanotubes, *J. Appl. Phys.*, vol. **96**(5), pp. 2864–2871, 2004.

Qian, D., Liu, W. K., and Ruoff, R. S., Mechanics of C_{60} in nanotubes, *J. Phys. Chem. B*, vol. **105**, pp. 10753–10758, 2001.

Qian, D., Liu, W. K., and Ruoff, R. S., Load transfer mechanism in carbon nanotube ropes, *Compos. Sci. Technol.*, vol. **63**(11), pp. 1561–1569, 2003.

Schadler, L. S., Giannaris, S. C., and Ajayan, P. M., Load transfer in carbon nanotube epoxy composites, *Appl. Phys. Lett.*, vol. **73**(26), pp. 3842–3844, 1998.

Sekar, C. and Subramanian, C., Purification and characterization of buckminsterfullerene, nanotubes and their by-products, *Vacuum*, vol. **47**(11), pp. 1289–1292, 1996.

Smith, W. and Forester, T. R., DL_POLY_2.0, A general-purpose parallel molecular dynamics simulation package, *J. Molec. Graphics*, vol. **14**(3), pp. 136–141, 1996.

Tagmatarchis, N., Georgakilas, V., Prato, M., and Shinohara, H., Sidewall functionalization of single-walled carbon nanotubes through electrophilic addition, *Chem. Commun.*, vol. **18**, pp. 2010–2011, 2002.

Wagner, H. D., Lourie, O., Feldman, Y., and Tenne, R., Stress-induced fragmentation of multiwall carbon nanotubes in a polymer matrix, *Appl. Phys. Lett.*, vol. **72**(2), pp. 188–190, 1998.

Wu, X. F. and Shi, G. Q., Synthesis of a carboxyl-containing conducting oligomer and non-covalent sidewall functionalization of single-walled carbon nanotubes, *J. Mater. Chem.*, vol. **15**(18), pp. 1833–1837, 2005.

Xu, Z., Chen, X., Qu, X. H., and Dong, S. J., Electrocatalytic oxidation of catechol at multi-walled carbon nanotubes modified electrode, *Electroanalysis*, vol. **16**(8), pp. 684–687, 2004.

Yumura, M., Ohshima, S., Uchida, K., Tasaka, Y., Kuriki, Y., Ikazaki, F., Saito, Y., and Uemura, S., Synthesis and purification of multiwalled carbon nanotubes for field emitter applications, *Diamond Relat. Mater.*, vol. **8**(2–5), pp. 785–791, 1999.